

A STUDY ON IMPULSE NOISE AND ITS MODELS

Thokozani Shongwe * and A. J. Han Vinck † and Hendrik C. Ferreira ‡

* Department of Electrical and Electronic Engineering Science, University of Johannesburg, P.O. Box 524, Auckland Park, 2006, Johannesburg, South Africa E-mail: tshongwe@uj.ac.za

† University of Duisburg-Essen, Institute for Experimental Mathematics, Ellernstr. 29, 45326 Essen, Germany E-mail: vinck@iem.uni-due.de

‡ Department of Electrical and Electronic Engineering Science, University of Johannesburg, P.O. Box 524, Auckland Park, 2006, Johannesburg, South Africa E-mail: hcferreira@uj.ac.za

Abstract: This article gives an overview of impulse noise and its models, and points out some important and interesting facts about the study of impulse noise which are sometimes overlooked or not well understood. We discuss the different impulse noise models in the literature, focusing on their similarities and differences when applied in communications systems. The impulse noise models discussed are memoryless (Middleton Class A, Bernoulli-Gaussian and Symmetric alpha-stable), and with memory (Markov-Middleton and Markov-Gaussian). We then go further to give performance comparisons in terms of bit error rates for some of the variants of impulse noise models. We also compare the bit error rate performance of single-carrier (SC) and multi-carrier (MC) communications systems operating under impulse noise. It can be seen that MC is not always better than SC under impulse noise. Lastly, the known impulse noise mitigation schemes (clipping/nulling using thresholds, iterative based and error control coding methods) are discussed.

Key words: Impulse noise models, Multi-carrier modulation, Single-carrier modulation, Bernoulli-Gaussian, Middleton Class A, Symmetric alpha-stable distribution.

1. INTRODUCTION

The effects of impulse noise are experienced by most communications systems. There has been a lot of research pertaining to impulse noise, which involve modelling of the impulse noise phenomena and combating impulse noise in communications systems. Research articles addressing impulse noise and its effects are found across different fields in communications, some of which are electromagnetic interference, wireless communication, and recently powerline communication. We therefore see it necessary to bring a contribution which gives a general view of impulse noise in communications systems, from the different research fields. The purpose of this article is to give an overview of impulse noise, and point out some important and interesting facts about the study of impulse noise which are sometimes overlooked. We begin by looking at the earliest work on impulse noise modelling by Middleton [1, Chapter 11], in Section 2.. Then we go on to discuss the common impulse noise models in the literature, in Section 3., dividing them into those with memory and without memory. We also look at the application of these models with single-carrier and multi-carrier systems. Lastly, we give an overview of the currently known methods of combating impulse noise, in Section 4.. This article follows from the preliminary work in [2].

2. AN INTRODUCTION TO MIDDLETON NOISE MODEL

The phenomenon of impulse noise was first described in detail by Middleton [1, Chapter 11] in the 1960s, where he gave a model for impulse noise in communications

systems. To obtain the model, Middleton [1, Chapter 11] described impulsive noise in a system as consisting of sequences of pulses (or impulses), of varying duration and intensity, and with the individual pulses occurring more or less random in time. He went further to divide the origin of impulse noise into two categories: (a) Man-made, which is induced by other devices connected in a communications network and (b) naturally occurring, due to atmospheric phenomena and solar static which is due to thunder storms, sun spots etc. The man-made impulse noise was described as trains of non-overlapping pulses, such as those in pulse time modulation. The impulse noise due to natural phenomena was described as the random superposition of the effects of the individual natural phenomena [1, Chapter 11]. A model for such noise is given in [3], [4] and [5] as

$$n(t) = \sum_{i=1}^L a_i \delta(t - t_i), \quad (1)$$

where

- $\delta(t - t_i)$ - is the i th unit (ideal) impulse, described as a delta function.
- a_i - are statistically independent with identical probability density functions (PDFs),
- t_i - are independent random variables uniformly distributed in the time period T_0 ,
- L - the number of impulses in any observation period T_0 , assumed to obey a Poisson distribution

$$P_{T_0}(L) = \frac{(\eta T_0)^L e^{-(\eta T_0)}}{L!}. \quad (2)$$

In (2), η is the average number of impulses per second, and T_0 is the observation period of the impulses. Therefore, ηT_0 is the average number of impulses in the period T_0 . It can be seen that the noise model described by (1) is ideal because the impulses are assumed to be delta functions, where $a_i \delta(t - t_i)$ describes the i_{th} impulse of amplitude a_i .

The noise model described by (1) and (2) was originally referred to as the Poisson noise model in [1, Chapter 11], and was widely studied and applied in many systems [3]–[6]. Ziemer [3], utilised the Poisson impulse noise model to calculate error probability characteristics of a matched filter receiver operating in an additive combination of impulsive and Gaussian noise. In [5], the Poisson noise model was used to evaluate the performance of noncoherent M -ary digital systems, ASK, PSK and FSK.

In his later work, Middleton [1] developed statistical noise models which catered for noise due to both man-made and natural phenomena [7]–[9]. In [7] Middleton classified the noise models into the following three categories: *Class A* – the noise has narrower bandwidth than that of the receiver; *Class B* – the noise has larger bandwidth than that of the receiver; *Class C* – the sum of Class A and Class B noise. The most famous of these noise models is the so-called Middleton Class A noise model, which has been widely accepted to model the effects of impulse noise in communications systems. We will, in short, refer to the Middleton Class A model as Class A model.

3. IMPULSE NOISE MODELS

Following Middleton’s noise models [1, Chapter 11], many authors studied impulse noise modelling. In this section, we discuss some impulse noise models found in the literature. In our discussion of the other impulse noise models we will occasionally mention the Middleton Class A model for reference or comparison purposes as it is a very important model in the study of impulse noise. To date, the following names appear in the literature for different impulse noise models:

1. Impulse noise models without memory

- Middleton Class A
- Bernoulli-Gaussian
- Symmetric Alpha-Stable distribution

2. Impulse noise models with memory

- Markov-Middleton
- Markov-Gaussian.

Impulse noise models without memory

3.1 Middleton Class A

The Class A noise model is still a form of the Poisson noise model, but with the impulse width taken into account in (2). We dedicate space to describing the Class A noise model because it has become the cornerstone of impulse noise modelling and has been extensively studied and utilised in the literature (see [10]–[17].) The Class A noise model gives the probability density function (PDF) of a noise sample, say n_k as follows:

$$F_M(n_k) = \sum_{m=0}^{\infty} P_m \mathcal{N}(n_k; 0, \sigma_m^2), \quad (3)$$

where

$\mathcal{N}(x_k; \mu, \sigma^2)$ represents a Gaussian PDF with mean μ and variance σ^2 , from which the k^{th} sample x_k is taken.

$$P_m = \frac{A^m e^{-A}}{m!} \quad (4)$$

and

$$\sigma_m^2 = \sigma_I^2 \frac{m}{A} + \sigma_g^2 = \sigma_g^2 \left(\frac{m}{A\Gamma} + 1 \right), \quad (5)$$

where σ_I^2 is the variance of the impulse noise and σ_g^2 is the variance of the background noise (AWGN). The parameter $\Gamma = \sigma_g^2 / \sigma_I^2$ gives the Gaussian to impulse noise power ratio. We can see that (2) and (4) are Poisson PDFs. The difference in (4) is that the term (ηT_0) has been replaced by the parameter A . The parameter A here represents the density of impulses (of a certain width) in an observation period. Therefore, $A = \eta \tau / T_0$, where η is the average number of impulses per second (as in (2)) and $T_0 = 1$, which is unit time. The new parameter τ , is the average duration of each impulse, where all impulses are taken to have the same duration. We now talk of density of impulses instead of number of impulses as done in (2). In (4) we therefore have the densities of impulse noise occurring according to a Poisson distribution.

The density is what has become accepted as “impulsive index”, A . The impulsive index is a parameter that is not well explained in the literature. We therefore give some details about the impulsive index, to enhance its understanding. It is worth stating that $A \leq 1$, this follows from the definition of impulsive index being a fraction of impulses in a given observation period T_0 . Therefore, for $\eta \tau > T_0$, the impulsive index is capped at 1 no matter how large $\eta \tau$ is, in the observation period T_0 .

Fig. 1 shows a pictorial view of the impulsive index, A , and what it means. Fig. 1 (a) shows η impulses each of duration τ , where the impulses occur in bursts (next to each other). In Fig. 1 (b) we show $\eta = 3$ impulses each of duration τ , where the impulses do not necessarily

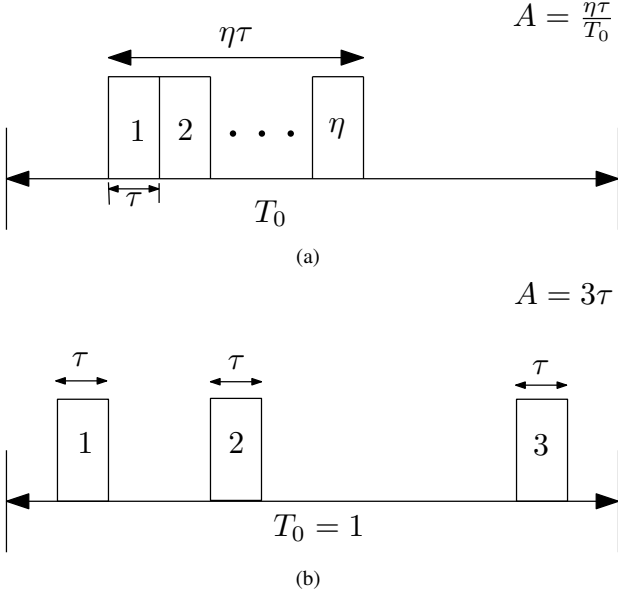


Figure 1: Example of Impulsive index: (a) Impulsive index (density) of η impulses, each with width (duration) τ , occupying a given time period T_0 and (b) impulsive index (density) of 3 impulses, each with width (duration) τ , occupying a given time period $T_0 = 1$.

occur in bursts. We also specify the period of observation as $T_0 = 1$ in Fig. 1 (b), which is usually the case in the calculation of the impulsive index. The conclusion drawn from Fig. 1 is that whether impulses occur in bursts or not, the calculation of the impulsive index follows the same procedure.

3.2 Bernoulli-Gaussian

The Middleton Class A noise model has already been explained. It can be seen that the PDF of the Class A noise model in (3) is a sum of different zero mean Gaussian PDFs with different variances σ_m^2 , where the PDFs are weighted by the Poisson PDF P_m . This summing of weighted Gaussian PDFs is generally referred to as a Gaussian mixture. Another popular impulse noise model, which is a Gaussian mixture according to the Bernoulli distribution, exists in the literature and is called the *Bernoulli-Gaussian* noise model (can be found in [18]–[21].) This noise model is described by the following PDF:

$$F_{BG}(n_k) = (1-p)\mathcal{N}(n_k; 0, \sigma_g^2) + p\mathcal{N}(n_k; 0, \sigma_g^2 + \sigma_I^2). \quad (6)$$

The Bernoulli-Gaussian noise model has similarities to the Class A noise model. To show the similarities, we use the channel models in Fig. 2. Fig. 2 (a) is a two-state representation of the Class A noise model, and Fig. 2 (b) is a representation the Bernoulli-Gaussian noise model. The models in Fig. 2 look very similar, with the only difference being that in Fig. 2 (b) it is explicitly stated that the noise sample added to the data symbol D_k , in either of the two

states, is Gaussian distributed. Whereas in Fig. 2 (a), only the state with variance σ_g^2 can have a Gaussian distribution. However, the state with impulse noise does not necessarily have a Gaussian distribution.

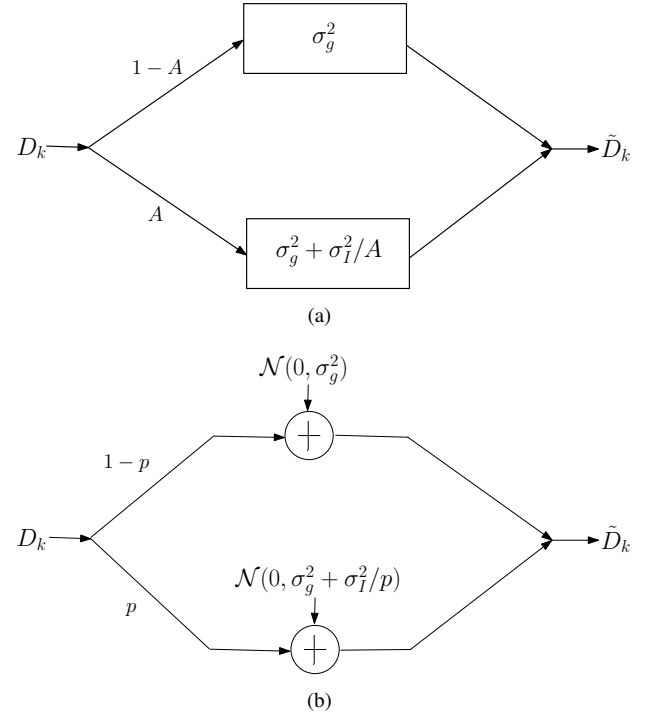


Figure 2: (a) Two-state Class A noise model and (b) Bernoulli-Gaussian noise model.

It should be noted that in the impulse noise model in Fig. 2, for the states with impulse noise, the impulse noise variance σ_I^2 is divided by the probability of entering into that state (A or p), such that the impulse noise variance in the system (total number of time samples) becomes σ_I^2 . To explain this, let us use the Class A noise model as follows: in the Class A noise model which is defined by (3)–(5), it can be seen that the impulse noise variance of the state m is $(\sigma_I^2 m)/A$ as shown in (5). This variance of state m occurs with probability P_m (see (4)), hence the average impulse noise variance of the Class A noise model is

$$\sum_{m=0}^{\infty} P_m \frac{\sigma_I^2 m}{A} = \frac{\sigma_I^2}{A} \sum_{m=0}^{\infty} m P_m = \frac{\sigma_I^2}{A} \times A = \sigma_I^2. \quad (7)$$

From a simulation point of view, we explain the division of σ_I^2 by A as follows: let us assume a transmission of N symbols. For the impulse noise variance, in the vector of length N , to be approximately σ_I^2 , each symbol has to be affected by impulse noise variance σ_I^2/A . It can easily be shown that this situation will result in the impulse noise of σ_I^2 over the N symbols, as follows: we know that impulse noise occurs with probability A , and for N symbols (assuming very large N) we have approximately AN symbols affected by impulse noise of variance σ_I^2/A . This gives the impulse noise variance in N samples as $\sigma_N^2 = AN \times \sigma_I^2/A = N\sigma_I^2$. Then the average impulse noise

variance is $\sigma_N^2/N = \sigma_I^2$, which is the result in (7). For the two models in Fig. 2 to be more similar, set $A = p$.

The Bernoulli-Gaussian noise model has been widely adopted in the literature, and some researchers prefer to employ it over the Class A noise model because it is more tractable than the Class A noise model. The Class A model has the advantage of having its parameters directly related to the physical channel. If so desired the Class A model can be adjusted to approximate the Bernoulli-Gaussian, hence giving the Bernoulli-Gaussian model the advantages of the Class A model as well.

The Class A model can also be simplified, and be made more manageable. It was shown in [11] that the PDF of the Class A noise model in (3) can be approximated by the first few terms of the summation and still be sufficiently accurate. Truncating (3) to the first K terms results in the approximation PDF (normalised), which is

$$F_{M,K}(n_k) = \sum_{m=0}^{K-1} P'_m \mathcal{N}(n_k; 0, \sigma_m^2), \quad (8)$$

where

$$P'_m = \frac{P_m}{\sum_{m=0}^{K-1} P_m}.$$

The model in (8) allowed Vastola [11] to design a threshold detector with a simpler structure, which would not have been the case if he was using the model in (3) which has infinite terms. It was also shown in [11] that the first two or three terms are good enough in (8) to approximate the PDF in (3). In [17], the first four terms were used to approximate the PDF of the Class A model. In our simulations, we shall use up to the first five terms of (8), and such a model is shown in Fig. 3.

We now give some results showing the bit error rate (BER) versus SNR when using the model in (8) for different K values. Such results are shown in Figs. 4 and 5, where BPSK modulation is used and $K = 2, 3$ and 5. In each figure, we use a theoretical BER curve for BPSK (given by (9) for $M = 2$, where M is the order of the PSK modulation and E_b is the signal's bit energy) as a reference curve against which all curves are compared. Figs. 4 and 5 show the effect of different values of A and Γ on the model.

$$P_{e,MPSK} = (1-A) \frac{M-1}{M} Q\left(\sqrt{\frac{E_b}{\sigma_g^2}}\right) + A \frac{M-1}{M} Q\left(\sqrt{\frac{E_b}{\sigma_g^2(1+1/AT)}}\right). \quad (9)$$

Note that the expression in (9) is normally written without the term $(M-1)/M$. However, for accuracy, the $(M-1)/M$ term needs to be included in the expression to indicate that a symbol affected by noise only gets to be in error with probability $(M-1)/M$. This is important

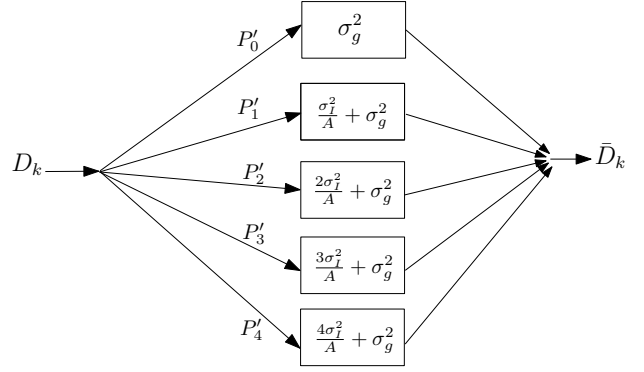


Figure 3: Five-term, $K = 5$, approximation of the Class A model.

for low order modulation, but can be neglected for higher order modulation because the term approaches one as M gets larger.

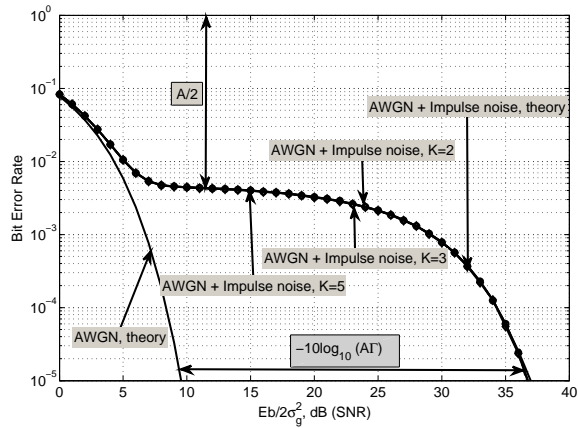
It can be observed in Figs. 4 and 5 that the model in (8) approximates the Class A model in (3) better for low values of A (see Fig. 4), such that even for two terms, $K = 2$, we get a very good approximation of the theoretical BER curve. For high values of A (see Fig. 5), however, we require more terms in (8) to approximate the results of the model in (3), at least for the part of the curve influenced by A (the error floor).

Fig. 5 shows that the results of the $K = 5$ channel model closely approximate the effect of A on the BER curve better than when $K = 2$. This is obviously due to the fact that the more terms (higher K values), the better the approximation of the Class A PDF. However, the $K = 2$ channel model results show a better approximation of the impulse noise power ($1/(A\Gamma)$), which is observed around a BER of 10^{-5}) compared to when $K = 5$. This is because of the m parameter in the term $\sigma_I^2 m/A$ in (5), which influences the impulse noise power. Using more terms in (8) to approximate the results of the model in (3) is more effective in estimating the effect of A in the BERs, but not the impulse noise power.

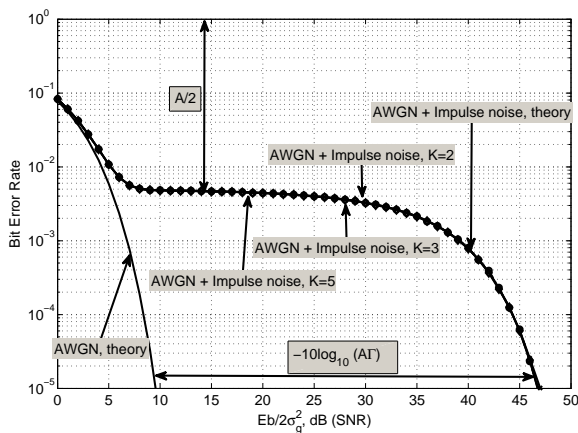
3.3 Symmetric α -stable distribution for impulse noise modelling

The impulse noise models discussed so far (the Middleton Class A and the Bernoulli-Gaussian) are by far the most widely used in the literature to model impulse noise. There is another impulse noise model that is becoming more common in the literature, and that is the symmetric α -stable (S α S) distribution. This section is therefore a short note on symmetric α -stable distributions used to model impulse noise.

S α S distributions are used in modelling phenomena encountered in practice. These phenomena do not follow the Gaussian distribution, instead their probability distributions may exhibit fat tails when compared to the Gaussian distribution tails [22, Chapter 1]. While stable distributions date back to the 1920s (see [23]), their usage



(a) $A = 0.01, \Gamma = 0.1$.



(b) $A = 0.01, \Gamma = 0.01$.

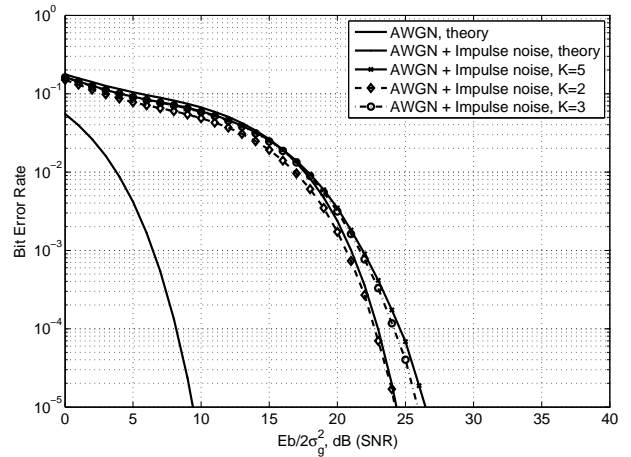
Figure 4: Bit error rate results using the impulse noise model shown in Fig. 3, with $K = 2, 3$ and 5 . BPSK was used for the modulation.

in practical applications had been limited until recently because of their lack of closed-form expressions except for a few (Levy, Cauchy and Gaussian distributions) [22, Chapter 1]. Nowadays powerful computer processors have made it possible to compute stable distributions despite the lack of closed form expressions. This has led to the increasing usage of stable distributions in modelling. Impulse noise is one phenomenon encountered in communication systems which has a probability distribution with fat tails [24]. $S\alpha S$ distributions are therefore considered appropriate for modelling impulse noise [24]– [27].

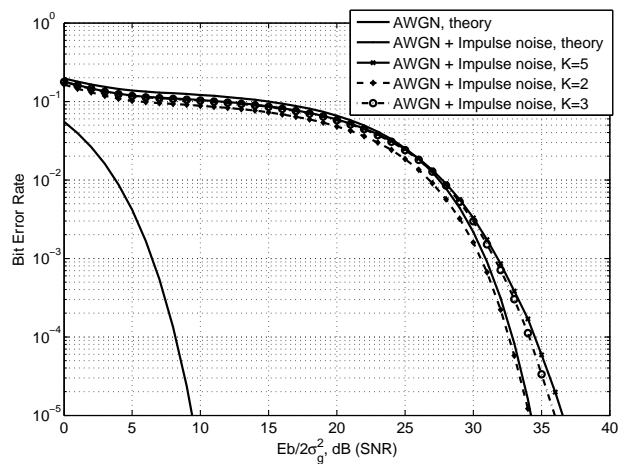
In this section we give examples of the PDFs of the $S\alpha S$ model for impulse noise, the Class A model and the Bernoulli-Gaussian model. This is meant to show how the $S\alpha S$ model compares, in terms of the PDFs, with the other impulse noise models already discussed.

The $S\alpha S$ distributions are characterised by the following parameters:

- α : is the characteristic exponent, and describes the



(a) $A = 0.3, \Gamma = 0.1$.



(b) $A = 0.3, \Gamma = 0.01$.

Figure 5: Bit error rate results using the impulse noise model shown in Fig. 3, with $K = 2, 3$ and 5 . BPSK was used for the modulation.

tail of the distribution ($1 < \alpha \leq 2$).

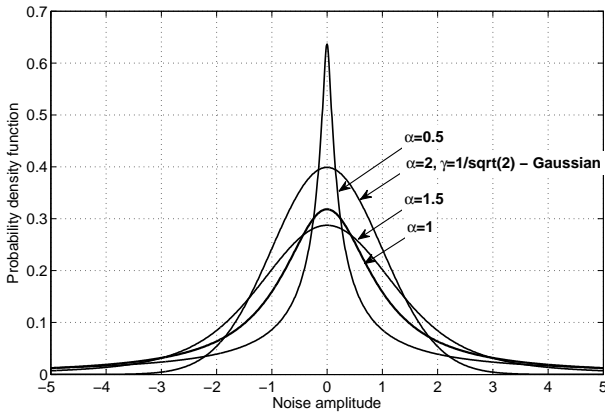
- β : describes the skewness of the distribution ($-1 \leq \beta \leq 1$); if the distribution is right-skewed ($\beta > 0$) or left-skewed ($\beta < 0$).
- γ : is the scaling parameter ($\gamma > 0$).
- δ : is a real number that gives the location of the distribution. This number tells us where the distribution is located on the x -axis (when the x -axis is used to represent the value of the random variable as per the norm).

The parameters α and β describe the shape of the distribution; while γ and δ can be thought of as similar to the variance and the mean in a Gaussian distribution, respectively, care should be taken when using these parameters as variance and mean.

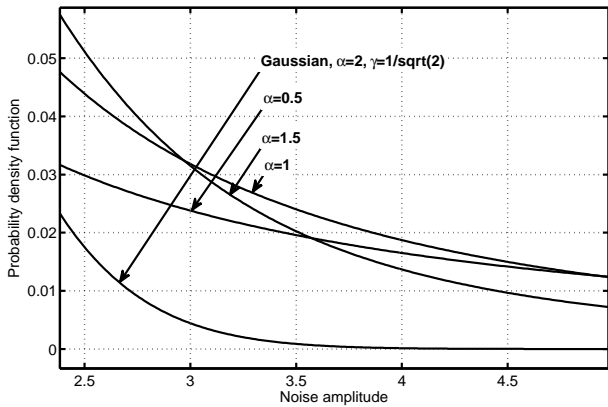
When modelling impulse noise using the $S\alpha S$ distribution, the noise is thought of as broadband noise, i.e., the

bandwidth of the noise is larger than that of the receiver [28]. Hence, the S α S distribution can be used in the place of the Middleton Class B noise model which requires more (six) parameters to be defined compared to the four parameters required to describe the S α S distribution.

Fig. 6 shows PDFs of the S α S models for different values of α while the other parameters are kept fixed ($\beta = 0$ and $\delta = 0$). The parameter γ is set at $\gamma = 1$ for all PDFs except for the $\alpha = 2$ PDF where $\gamma = 1/\sqrt{2}$. This case of $\alpha = 2$, $\gamma = 1/\sqrt{2}$, $\beta = 0$ and $\delta = 0$ results in the normal distribution as seen in Fig. 6. It should be noted that the S α S distribution of $\alpha = 2$, $\beta = 0$, $\delta = 0$ and $\gamma > 0$ is generally the Gaussian distribution; making the Gaussian distribution a special case of the S α S distributions. Our main aim of presenting Fig. 6 is to show the change of the tails of the S α S PDFs with change in the parameter α and show that the tails are fatter than that of the Gaussian distribution for $\alpha < 2$.



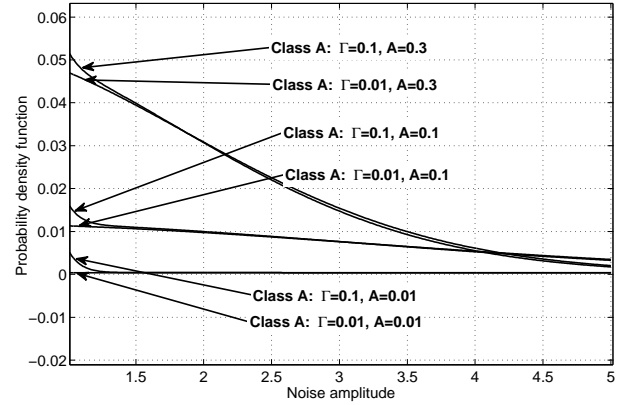
(a) S α S distributions



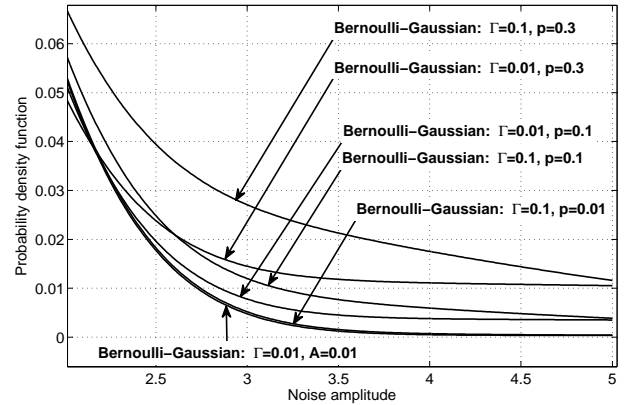
(b) Tails of the distributions

Figure 6: S α S distributions of different values of α while $\beta = 0$, $\gamma = 1$ and $\delta = 0$. The normal distribution is also included as a S α S distribution of $\alpha = 2$, $\beta = 0$, $\gamma = 1/\sqrt{2}$ and $\delta = 0$.

It can be seen in Figs. 6 and 7 that the PDFs of the impulse noise models (Bernoulli-Gaussian, Middleton Class A and S α S) have fat tails. For the Bernoulli-Gaussian and Middleton Class A PDFs, the tails are controlled by the probabilities of impulse noise p and A , respectively; when



(a) Tails of the PDFs of the Class A model



(b) Tails of the PDFs of the Bernoulli-Gaussian model

Figure 7: Tails of the PDFs of the Class model for different values of A and Γ ; tails of the PDFs of the Bernoulli-Gaussian model for different values of p and Γ .

the probability of impulse noise (p or A) increases, the PDFs tails get fatter. For the S α S PDF, the tails are controlled by the parameter α ; with low values of α ($\alpha < 2$) giving PDFs with fatter tails.

Impulse noise models with memory

Through measurements in a practical communications channel, Zimmermann and Dostert [29] showed that impulse noise samples sometimes occur in bursts, hence presenting a channel with memory. They further proposed a statistical impulse noise model, based on a partitioned Markov chain, that takes into account the memory nature of impulse noise. Following the work in [29], other authors studied impulse noise with memory as seen in [30], [31], [17] and [32]. In [30], a two-layer two-state Markov model is used to describe bursty impulse noise. The first layer uses a two-state Markov chain to describe the occurrence of impulses and the second layer uses another two-state Markov chain to describe the behaviour of a single impulse. To model impulse noise with memory, Markov chains are invariably used by most authors in the literature. The two models, *Markov-Middleton* [17] and *Markov-Gaussian* [31] are modifications of the Class A and Bernoulli-Gaussian models, respectively, by including

Markov chains. Having discussed the impulse noise models without memory, there is no need for a lengthy discussion about the impulse noise models with memory. This is because the impulse noise models with memory are founded on those models without memory. In Fig. 8 we show Markov-Middleton models, which means Class A model with memory. These models in Fig. 8 are an adaptation of the model shown in Fig. 3. The model in Fig. 8 (a) is a “direct” adaptation of the one in Fig. 3, with all the parameters unchanged except for the introduction of memory. However, the model in Fig. 8 (b) [17] allows for all states to be connected such that it is possible to move from one bad state (state with impulse noise) to another bad state, which was not possible with the models in Fig. 3 and Fig. 8 (a). With this modification, in Fig. 8 (b), comes a new parameter x , which is independent of the Class A model parameters A , Γ and σ_I^2 . The parameter x describes the time correlation between noise samples. The transition state in Fig. 8 (b) has no time duration, it facilitates the connection of the other states. It was shown in [17] that the PDF of their model in Fig. 8 (b) is equivalent to that of Class A model shown in (8).

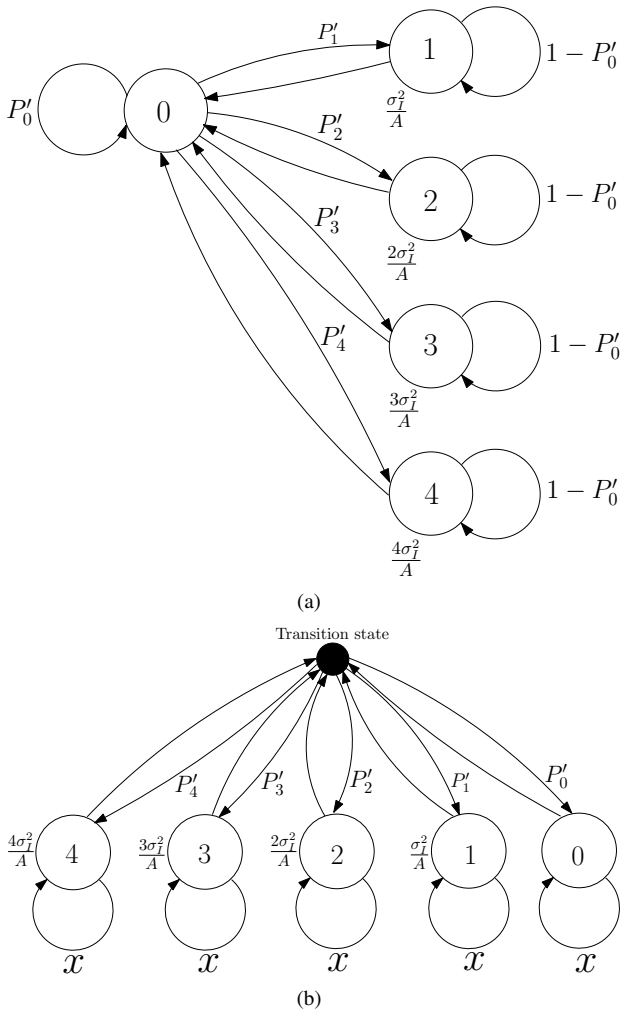


Figure 8: Markov-Middleton impulse noise models with five terms: (a) is adapted from [33] and (b) is adapted from [17]

A Note on Multi-carrier and Single-carrier modulation with Impulse noise

Many authors may correctly argue that the short fall of the Class A and Bernoulli-Gaussian noise models is that they do not take into account the bursty nature of impulse noise. However, for MC modulation it does not matter whether the noise model employed has memory or is memoryless. This is because in MC modulation, the transform (DFT) spreads the time domain impulse noise on all the subcarriers in the frequency domain such that it becomes irrelevant how the noise occurred (in bursts or randomly). This is well explained by Suraweera and Armstrong [34], who showed that the degradation caused by impulse noise in OFDM systems depends only on the total noise energy within one OFDM symbol period, not on the detailed distribution of the noise energy within the symbol. When it comes to SC modulation, however, it may be important to distinguish impulse noise with and without memory.

Here we employ the two-state Class A memoryless model in Fig. 2 (a), with the PDF of the state with impulse noise and AWGN being Gaussian. This makes the model more similar to the Bernoulli-Gaussian in Fig. 2 (b). In this two-state Class A model, ignoring the effect of the background noise for a moment, we know that the average impulse noise power is $\sigma_I^2 = \sigma_g^2/\Gamma$. The impulse noise power affecting a symbol is $\bar{\sigma}_I^2 = \sigma_I^2/A = \sigma_g^2/A\Gamma$. For discussions and analysis, we will be using the impulse noise power $\bar{\sigma}_I^2 = \sigma_g^2/A\Gamma$.

Given a fixed impulse noise power $\bar{\sigma}_I^2 = \sigma_g^2/A\Gamma$, we vary impulse noise probability A and the impulse noise strength Γ such that $\bar{\sigma}_I^2$ remains the same. This means that if we lower A by a certain amount, we have to increase Γ by the same amount such that the product $A\Gamma$ is unchanged. This we do in order to keep $\bar{\sigma}_I^2$ the same, while observing the effect of changing the probability of impulse noise A on the performance of Single-Carrier and Multi-Carrier Modulation. It is interesting to note that for very low A , SC modulation performs better in the low SNR region compared to MC modulation. However, SC modulation gives an error floor, while MC modulation does not. This behaviour is seen in Fig. 9.

Two important conclusions can be drawn from the behaviour observed in Fig. 9:

- For very low A , very few symbols are affected in SC modulation, hence the low probability of error in SC no matter the strength (or average variance) of the impulse noise. However, with MC modulation, what matters is the average impulse noise variance in the system because the noise power is spread on all subcarriers causing every symbol to be affected by the impulse noise.
- MC modulation has the benefit of eventually outperforming SC modulation as the SNR increases.

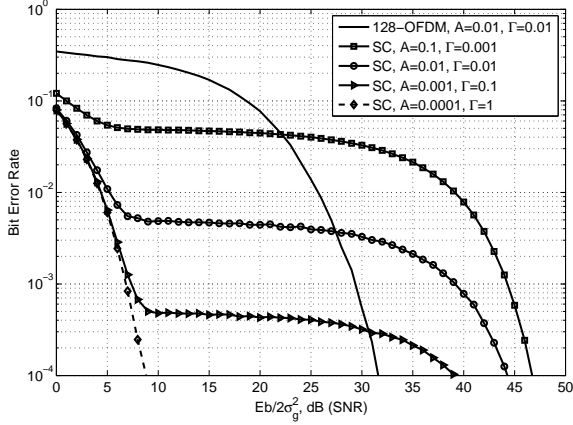


Figure 9: Comparison of MC and SC modulation in a channel with AWGN and impulse noise of variance $\sigma_g^2 = \sigma_g^2 / A\Gamma = 1 / (0.01 \times 0.01) = 10^4$. σ_g^2 is fixed at 10^4 while different values of A (10^{-1} , 10^{-2} , 10^{-3} and 10^{-4}) are seen to influence the performance of SC modulation.

This is because with MC modulation, the factor $1/A$ does not affect the SNR requirement like in SC modulation. We show this independence on A in MC modulation in Fig. 10.

From the two points above, we can say that MC modulation's performance is independent on the probability of impulse noise occurrence A , while SC modulation's performance shows a strong dependence on A . Therefore, one has to carefully choose between MC and SC modulation depending on the probability of impulse noise that can be tolerated in the communication. By this we mean that if, for example in Fig. 9, $A = 10^{-4}$ and communication is acceptable at probability of error of 10^{-4} , then SC modulation will be the best choice over MC modulation because it will only give an error floor just below A , at $A(M-1)/M$. Ghosh [18] also mentioned that there are conditions where SC modulation performs better than MC modulation. It was also shown in [19], using the Bernoulli-Gaussian noise model, that the impact of impulse noise on the information rate of SC schemes is negligible as long as the occurrence of an impulse noise event is sufficiently small (i.e. very low p in (6)).

4. COMBATING IMPULSE NOISE

Several techniques for combating impulse noise have been presented in the literature. We shall discuss these techniques in light of MC modulation, OFDM. These techniques fall into the following three broad categories:

1. Clipping and Nulling (or Blanking):

With clipping or nulling, a threshold T_h is used to detect impulse noise in the received signal vector \mathbf{r} before demodulation. Clipping and nulling differ in the action taken when impulse noise is detected in \mathbf{r} . If a sample of \mathbf{r} , r_k is detected to be corrupted

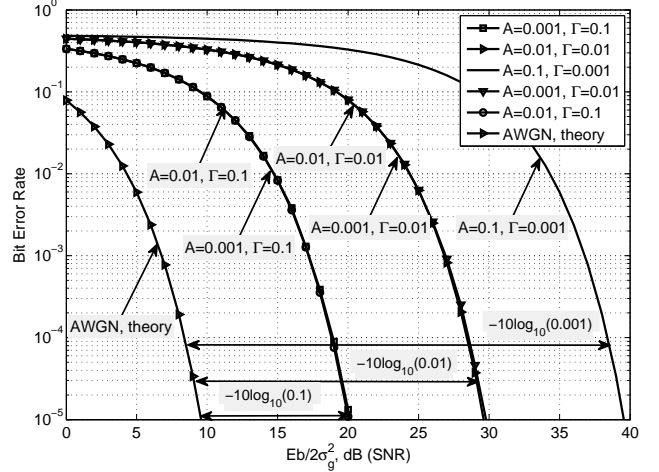


Figure 10: Shows that with MC modulation the SNR requirement is $\sigma_g^2 = 1/\Gamma$ instead of $1/A\Gamma$, even though a symbol is affected by impulse noise of variance σ_g^2/A . BPSK OFDM was used, with a DFT size of 10000.

with impulse noise, its magnitude is clipped/limited according to $T_h = T_{\text{clip}}$ (Clipping), or set to zero (Nulling) according to $T_h = T_{\text{null}}$. Given the received sample r_k , then the resulting sample \tilde{r}_k , from the clipping technique, is given by

$$\tilde{r}_k = \begin{cases} r_k, & \text{for } |r_k| \leq T_{\text{clip}} \\ T_{\text{clip}} e^{j\arg(r_k)}, & \text{for } |r_k| > T_{\text{clip}} \end{cases},$$

and the resulting sample \tilde{r}_k , from the nulling technique, is given by

$$\tilde{r}_k = \begin{cases} r_k, & \text{for } |r_k| \leq T_{\text{null}} \\ 0, & \text{for } |r_k| > T_{\text{null}} \end{cases},$$

where usually $T_{\text{clip}} < T_{\text{null}}$.

Zhidkov [35] gave performance analysis and optimization of blanking (or nulling) for OFDM receivers in the presence of impulse noise, as well as a comparison of clipping, blanking, and combined clipping and blanking in [36]. In [37], the authors advocated for the clipping technique to combat impulse noise in digital television systems using OFDM. The clipping technique, in OFDM, is also seen in [38], where the focus is on deriving and utilising a clipping threshold that does not require the a priori knowledge of the PDF of impulse noise. Recently, Papilaya and Vinck [39] proposed to include an additional action (with its threshold) to the clipping and nulling actions, which is termed *replacement*. This was done for an OFDM system. The replacement action uses a replacement threshold (T_{rep}) which falls in between the clipping and nulling thresholds, and replaces impulse corrupted samples with the average magnitude of the noiseless OFDM samples.

2. Iterative:

With the iterative technique, the idea is to estimate

is obviously because the demodulator in SC modulation does not discriminate between high and low amplitude noise when making a decision on the transmitted symbol. The benefit of clipping and/or nulling impulse noise affected samples, in SC modulation is observed when performing soft-decision decoding. Impulse noise in SC modulation has the same effect as narrow-band interference (NBI) in OFDM, considering the NBI model in [49]. Therefore, the same techniques of handling NBI in OFDM found in [49], clipping and/or nulling and error correcting coding, can be used to handle impulse noise in SC modulation. It was shown in [49] that the best technique that gives optimal performance when using a convolutional decoder, is to combine nulling and convolutional soft-decision decoding. Combining clipping and convolutional soft-decision decoding gives suboptimal performance. Impulse noise in SC modulation can be handled exactly the same way. If the impulse noise has memory, the classical interleaver can be employed to randomise the occurrence of errors, hence improving the decoded BER performance.

Focusing on the PLC channel, Vinck [50] proposed the use of a combination of permutation codes and MFSK, to combat impulse noise, as well as other noise types in the PLC channel. This technique was applied in SC modulation, MFSK. Later on, the idea of employing permutation codes with MFSK, in [50], to combat noise typical for a PLC channel (including impulse noise) was taken further in [51] and [52], where powerful permutation codes (called permutation trellis codes) were constructed and used not only to combat impulse noise.

Other impulse noise combating techniques

Another technique used to combat impulse noise in OFDM systems is compressed (or compressive) sensing (CS). With compressed sensing, the idea is to reconstruct a digitized signal using a few of its samples. CS works well with sparse signals. Using CS, the impulse noise in an OFDM signal can be estimated by using pilot subcarriers with their values set to zero. We see the idea of using CS to estimate and cancel impulse noise in OFDM in [53]. In [54] the authors proposed channel estimation working in conjunction with compressed sensing to combat impulse noise for OFDM based power line communication systems. While most research on combating impulse noise focuses on non-bursty impulse noise, Lampe [55] proposed a CS based impulse noise mitigation technique for OFDM that can detect bursty impulse noise. After detecting the impulse noise positions in the OFDM samples, impulse noise cancellation or suppression was applied.

Another technique for combating impulse noise in OFDM, which is similar to compressed sensing, is using the similarity between the DFT (in OFDM) and error correcting codes (particularly Bose-Chaudhuri-Hocquengem and Reed-Solomon codes). This idea, of using the similarities between the DFT and error correcting codes to combat impulse noise, dates back to the 80s where we see Wolf [56] showing that the DFT sequence carries redundant

information which can be used to detect and correct errors. Wolf [56] compared the DFT to BCH codes. In [57] the authors show that the OFDM modulator is similar to a Reed-Solomon (RS) encoder and these similarities can be used in OFDM to cancel impulse noise effects. While the scheme in [57] could correct a very limited number of impulse errors because the limitation imposed by the amount of redundancy, an improved scheme with better correcting capabilities was proposed by Mengi and Vinck [58]. The Mengi and Vinck [58] scheme also used OFDM as a RS code, where they proposed to observe not only the subcarriers containing the redundancy symbols but the subcarriers containing information symbols as well. That way their scheme could correct more impulse errors.

5. CONCLUSION

Our conclusion is mainly a summary of the interesting facts about impulse noise models. We have also included Table 1 to summarise some of the important features of the noise models. It should be noted that in Table 1 the bandwidth of the noise is narrow or broad in reference to the bandwidth of the receiver.

Table 1: Summary of the features of the impulse noise models.

	Class A	Bernoulli-Gaussian	$S\alpha S$
Noise Bandwidth	Narrow-band	not specified	Broad-band
Closed-form expression	exists	exists	does not exist
PDF	exhibits fat tails	exhibits fat tails	exhibits fat tails
Bursty noise modelling	as Markov-Middleton	as Markov-Gaussian	does not model bursty noise

In this article we have discussed some important impulse noise models found in the literature. The noise models are divided into those without memory (Middleton Class A and Bernoulli-Gaussian) and those with memory (Markov-Middleton and Markov-Gaussian). We went further to look at the approximation of the PDF of the Middleton Class A model with five terms. We also showed that the Bernoulli-Gaussian model has similarities with the Middleton Class A, and it can be approximated with the Middleton Class A model. We then showed Bit error rate simulation results of the approximation of the Middleton Class A with five terms. Using the Middleton Class A model with five terms we showed equivalent Markov-Middleton models. In addition to the Middleton Class A and Bernoulli-Gaussian models, we also discussed the symmetric alpha(α)-stable distribution used to model impulse noise. The Symmetric alpha(α)-stable distribution as an impulse noise model was compared with the PDFs of the Middleton Class A and Bernoulli-Gaussian models. All the three models had PDFs that exhibit fat tails. We also showed that single-carrier modulation performs better than multi-carrier modulation under low probability of impulse noise occurrence. With OFDM transmission,

it is irrelevant whether the noise occurred in bursts or randomly, what matters is the total noise energy within one OFDM symbol period. Lastly, we discussed impulse noise mitigation schemes: clipping, nulling, iterative and error correcting coding.

ACKNOWLEDGMENTS

The authors would like to thank Alliander, Netherlands for partially funding this work. This work is also a successful outcome of the cooperation between University of Johannesburg (South Africa) and Duisburg-Essen University (Germany).

REFERENCES

- [1] D. Middleton, *An introduction to statistical communication theory*. McGraw-Hill New York, 1960, vol. 960.
- [2] T. Shongwe, A. J. H. Vinck, and H. C. Ferreira, "On impulse noise and its models," in *Proceedings of the 2014 IEEE International Symposium on Power Line Communications*, 2014, pp. 12–17.
- [3] R. Ziemer, "Error probabilities due to additive combinations of Gaussian and impulsive noise," *IEEE Transactions on Communication Technology*, vol. 15, no. 3, pp. 471–474, June 1967.
- [4] —, "Character error probabilities for M-ary signaling in impulsive noise environments," *IEEE Transactions on Communication Technology*, vol. 15, no. 1, pp. 32–34, Feb. 1967.
- [5] H. Huynh and M. Lecours, "Impulsive noise in noncoherent M-ary digital systems," *IEEE Transactions on Communications*, vol. 23, no. 2, pp. 246–252, Feb. 1975.
- [6] S. A. Kosmopoulos, P. T. Mathiopoulos, and M. D. Gouta, "Fourier-Bessel error performance analysis and evaluation of M-ary QAM schemes in an impulsive noise environment," *IEEE Transactions on Communications*, vol. 39, no. 3, pp. 398–404, Mar. 1991.
- [7] D. Middleton, "Statistical-physical models of electromagnetic interference," *IEEE Transactions on Electromagnetic Compatibility*, vol. 19, no. 3, pp. 106–127, Aug. 1977.
- [8] —, "Procedures for determining the parameters of the first-order canonical models of class A and class B electromagnetic interference," *IEEE Transactions on Electromagnetic Compatibility*, vol. 21, no. 3, pp. 190–208, Aug. 1979.
- [9] —, "Canonical and quasi-canonical probability models of class A interference," *IEEE Transactions on Electromagnetic Compatibility*, vol. 25, no. 2, pp. 76–106, May 1983.
- [10] L. A. Berry, "Understanding Middleton's canonical formula for class A noise," *IEEE Transactions on Electromagnetic Compatibility*, vol. 23, no. 4, pp. 337–344, Nov. 1981.
- [11] K. Vastola, "Threshold detection in narrow-band non-Gaussian noise," *IEEE Transactions on Communications*, vol. 32, no. 2, pp. 134–139, Feb. 1984.
- [12] S. Miyamoto, M. Katayama, and N. Morinaga, "Performance analysis of QAM systems under class A impulsive noise environment," *IEEE Transactions on Electromagnetic Compatibility*, vol. 37, no. 2, pp. 260–267, May 1995.
- [13] J. Häring and A. J. H. Vinck, "OFDM transmission corrupted by impulsive noise," in *Proceedings of the 2000 International Symposium on Power-Line Communications and its Applications*, Limerick, Ireland, Apr. 5–7, 2000, pp. 5–7.
- [14] —, "Performance bounds for optimum and suboptimum reception under Class-A impulsive noise," *IEEE Transactions on Communications*, vol. 50, no. 7, pp. 1130–1136, July 2002.
- [15] —, "Iterative decoding of codes over complex numbers for impulsive noise channels," *IEEE Transactions on Information Theory*, vol. 49, no. 5, pp. 1251–1260, May 2003.
- [16] K. C. Wiklundh, P. F. Stenumgaard, and H. M. Tullberg, "Channel capacity of Middleton's class A interference channel," *Electronics letters*, vol. 45, no. 24, pp. 1227–1229, Nov. 2009.
- [17] G. Ndo, F. Labeau, and M. Kassouf, "A Markov-Middleton model for bursty impulsive noise: Modeling and receiver design," *IEEE Transactions on Power Delivery*, vol. 28, no. 4, pp. 2317–2325, Oct. 2013.
- [18] M. Ghosh, "Analysis of the effect of impulse noise on multicarrier and single carrier QAM systems," *IEEE Transactions on Communications*, vol. 44, no. 2, pp. 145–147, Feb. 1996.
- [19] R. Pighi, M. Franceschini, G. Ferrari, and R. Raheli, "Fundamental performance limits of communications systems impaired by impulse noise," *IEEE Transactions on Communications*, vol. 57, no. 1, pp. 171–182, Jan. 2009.
- [20] T. Y. Al-Naffouri, A. A. Quadeer, and G. Caire, "Impulsive noise estimation and cancellation in DSL using orthogonal clustering," in *Proceedings of the 2005 IEEE International Symposium on Information Theory*, Saint Petersburg, Russia, July 31–Aug. 5, 2011, pp. 2841–2845.
- [21] S. P. Herath, N. H. Tran, and T. Le-Ngoc, "On optimal input distribution and capacity limit of Bernoulli-Gaussian impulsive noise channels," in *Proceedings of the 2012 IEEE International*

Conference on Communications, Ottawa, ON, Canada, June 10–15, 2012, pp. 3429–3433.

- [22] J. P. Nolan, *Stable Distributions: Models for Heavy-Tailed Data*. Boston: Birkhauser, 2007.
- [23] P. Levy, *Calcul des Probabilites*. Paris: Gauthier-Villars, 1925.
- [24] C. L. Brown and A. M. Zoubir, “A nonparametric approach to signal detection in impulsive interference,” *IEEE Transactions on Signal Processing*, vol. 48, no. 9, pp. 2665–2669, 2000.
- [25] G. A. Tsihrintzis and C. L. Nikias, “Performance of optimum and suboptimum receivers in the presence of impulsive noise modeled as an alpha-stable process,” *IEEE Transactions on Communications*, vol. 43, no. 234, pp. 904–914, 1995.
- [26] E. E. Kuruoglu, W. J. Fitzgerald, and P. J. Rayner, “Near optimal detection of signals in impulsive noise modeled with a symmetric α -stable distribution,” *IEEE Communications Letters*, vol. 2, no. 10, pp. 282–284, 1998.
- [27] J. Ilow and D. Hatzinakos, “Analytic alpha-stable noise modeling in a poisson field of interferers or scatterers,” *IEEE Transactions on Signal Processing*, vol. 46, no. 6, pp. 1601–1611, 1998.
- [28] D. Middleton, “Non-Gaussian noise models in signal processing for telecommunications: new methods and results for class A and class B noise models,” *IEEE Transactions on Information Theory*, vol. 45, no. 4, pp. 1129–1149, 1999.
- [29] M. Zimmermann and K. Dostert, “Analysis and modeling of impulsive noise in broad-band powerline communications,” *IEEE Transactions on Electromagnetic Compatibility*, vol. 44, no. 1, pp. 249–258, Feb. 2002.
- [30] P. Amirshahi, M. S. Navidpour, and M. Kavehrad, “Performance analysis of uncoded and coded OFDM broadband transmission over low voltage power-line channels with impulsive noise,” *IEEE Transactions on Power Delivery*, vol. 21, no. 4, pp. 1927–1934, Oct. 2006.
- [31] D. Fertoni and G. Colavolpe, “On reliable communications over channels impaired by bursty impulse noise,” *IEEE Transactions on Communications*, vol. 57, no. 7, pp. 2024–2030, July 2009.
- [32] J. Mitra and L. Lampe, “Convolutionally coded transmission over Markov-Gaussian channels: Analysis and decoding metrics,” *IEEE Transactions on Communications*, vol. 58, no. 7, pp. 1939–1949, July 2010.
- [33] H. C. Ferreira, L. Lampe, J. Newbury, and T. G. Swart, *Power Line Communications: Theory and Applications for Narrowband and Broadband Communications Over Power Lines*. Chichester, England: John Wiley and Sons, 2010.
- [34] H. A. Suraweera and J. Armstrong, “Noise bucket effect for impulse noise in OFDM,” *Electronics Letters*, vol. 40, no. 18, pp. 1156–1157, Sept. 2004.
- [35] S. V. Zhidkov, “Performance analysis and optimization of OFDM receiver with blanking nonlinearity in impulsive noise environment,” *IEEE Transactions on Vehicular Technology*, vol. 55, no. 1, pp. 234–242, Jan. 2006.
- [36] —, “Analysis and comparison of several simple impulsive noise mitigation schemes for OFDM receivers,” *IEEE Transactions on Communications*, vol. 56, no. 1, pp. 5–9, Jan. 2008.
- [37] H. A. Suraweera, C. Chai, J. Shentu, and J. Armstrong, “Analysis of impulse noise mitigation techniques for digital television systems,” in *Proceedings the 8th international OFDM Workshop*, Hamburg, Germany, Sept. 2003, pp. 172–176.
- [38] D.-F. Tseng, Y. S. Han, W. H. Mow, L.-C. Chang, and A. J. H. Vinck, “Robust clipping for OFDM transmissions over memoryless impulsive noise channels,” *IEEE Communications Letters*, vol. 16, no. 7, pp. 1110–1113, July 2012.
- [39] V. N. Papilaya and A. J. H. Vinck, “Investigation on a new combined impulsive noise mitigation scheme for OFDM transmission,” in *Proceedings of the 2013 IEEE International Symposium on Power Line Communications*, Johannesburg, South Africa, Mar. 24–27, 2013, pp. 86–91.
- [40] S. V. Zhidkov, “Impulsive noise suppression in OFDM-based communication systems,” *IEEE Transactions on Consumer Electronics*, vol. 49, no. 4, pp. 944–948, Nov. 2003.
- [41] D. H. Sargrad and J. W. Modestino, “Errors-and-erasures coding to combat impulse noise on digital subscriber loops,” *IEEE Transactions on Communications*, vol. 38, no. 8, pp. 1145–1155, Aug. 1990.
- [42] T. Li, W. H. Mow, and M. Siu, “Joint erasure marking and viterbi decoding algorithm for unknown impulsive noise channels,” *IEEE Transactions on Wireless Communications*, vol. 7, no. 9, pp. 3407–3416, Sept. 2008.
- [43] T. Faber, T. Scholand, and P. Jung, “Turbo decoding in impulsive noise environments,” *Electronics letters*, vol. 39, no. 14, pp. 1069–1071, July 2003.
- [44] A. Burnic, A. Hessamian-Alinejad, T. Scholand, T. E. Faber, G. H. Bruck, and P. Jung, “Error correction in impulsive noise environments by applying turbo codes,” in *Proceedings of the 2006 IEEE International Symposium on Personal, Indoor and Mobile Radio Communications*, Helsinki, Finland, Sept. 11–14, 2006, pp. 1–5.

- [45] H. Nakagawa, D. Umehara, S. Denno, and Y. Morihira, "A decoding for low density parity check codes over impulsive noise channels," in *Proceedings of the 2005 International Symposium on Power Line Communications*, Vancouver, Canada, Apr. 6–8, 2005, pp. 85–89.
- [46] H.-M. Oh, Y.-J. Park, S. Choi, J.-J. Lee, and K.-C. Whang, "Mitigation of performance degradation by impulsive noise in ldpc coded ofdm system," in *Proceedings of the 2006 IEEE International Symposium on Power Line Communications*, Orlando, Florida, USA, Mar. 26–29, 2006, pp. 331–336.
- [47] A. Mengi and A. J. H. Vinck, "Successive impulsive noise suppression in OFDM," in *Proceedings of the 2009 IEEE International Symposium on Power Line Communications*, Rio de Janeiro, Brazil, Mar. 5–7, 2009, pp. 33–37.
- [48] C.-H. Yih, "Iterative interference cancellation for OFDM signals with blanking nonlinearity in impulsive noise channels," *IEEE Signal Processing Letters*, vol. 19, no. 3, pp. 147–150, Mar. 2012.
- [49] T. Shongwe and A. J. H. Vinck, "Interleaving and nulling to combat narrow-band interference in PLC standard technologies PLC G3 and PRIME," in *Proceedings of the 2013 IEEE International Symposium on Power Line Communications*, Johannesburg, South Africa, Mar. 24–27, 2013, pp. 258–262.
- [50] A. J. H. Vinck, "Coded modulation for powerline communications," *AEÜ International Journal of Electronics and Communications*, vol. 54, no. 1, pp. 45–49, Jan. 2000.
- [51] H. C. Ferreira and A. J. H. Vinck, "Interference cancellation with permutation trellis codes," in *Proceedings of the 2000 IEEE Vehicular Technology Conference*, Boston, MA, USA, Sept. 24–28, 2000, pp. 2401–2407.
- [52] H. C. Ferreira, A. J. H. Vinck, T. G. Swart, and I. de Beer, "Permutation trellis codes," *IEEE Transactions on Communications*, vol. 53, no. 11, pp. 1782–1789, Nov. 2005.
- [53] G. Caire, T. Y. Al-Naffouri, and A. K. Narayanan, "Impulse noise cancellation in ofdm: an application of compressed sensing," in *Proceedings of the 2008 IEEE International Symposium on Information Theory*, Toronto, ON, Canada, July 6–11, 2008, pp. 1293–1297.
- [54] A. Mehboob, L. Zhang, J. Khangosstar, and K. Suwunnapak, "Joint channel and impulsive noise estimation for OFDM based power line communication systems using compressed sensing," in *Proceedings of the 2013 IEEE International Symposium on Power Line Communications*, Johannesburg, South Africa, Mar. 24–27, 2013, pp. 203–208.
- [55] L. Lampe, "Bursty impulse noise detection by compressed sensing," in *Proceedings of the 2011 IEEE International Symposium on Power Line Communications*, Udine, Italy, Apr. 3–6, 2011, pp. 29–34.
- [56] J. Wolf, "Redundancy, the discrete Fourier transform, and impulse noise cancellation," *IEEE Transactions on Communications*, vol. 31, no. 3, pp. 458–461, Mar. 1983.
- [57] F. Abdelkefi, P. Duhamel, and F. Alberge, "Impulsive noise cancellation in multicarrier transmission," *IEEE Transactions on Communications*, vol. 53, no. 1, pp. 94–106, Jan. 2005.
- [58] A. Mengi and A. J. H. Vinck, "Impulsive noise error correction in 16-OFDM for narrowband power line communication," in *Proceedings of the 2009 IEEE International Symposium on Power Line Communications*, Dresden, Germany, Mar. 29–Apr. 1, 2009, pp. 31–35.